

11/30/94

SANDIA REPORT

SAND94-2368 • UC-722

Unlimited Release

Printed October 1994

Simulation of Impact of the Generic Accident-Resistant Packaging (GAP)

Adam M. Slavin

Prepared by
Sandia National Laboratories
Albuquerque, New Mexico 87185 and Livermore, California 94550
for the United States Department of Energy
under Contract DE-AC04-94AL85000

Approved for public release; distribution is unlimited.

MASTER *ds*

DISTRIBUTION OF THIS DOCUMENT IS UNLIMITED DEC 13 1994

DISCLAIMER

This report was prepared as an account of work sponsored by an agency of the United States Government. Neither the United States Government nor any agency thereof, nor any of their employees, make any warranty, express or implied, or assumes any legal liability or responsibility for the accuracy, completeness, or usefulness of any information, apparatus, product, or process disclosed, or represents that its use would not infringe privately owned rights. Reference herein to any specific commercial product, process, or service by trade name, trademark, manufacturer, or otherwise does not necessarily constitute or imply its endorsement, recommendation, or favoring by the United States Government or any agency thereof. The views and opinions of authors expressed herein do not necessarily state or reflect those of the United States Government or any agency thereof.

DISCLAIMER

Portions of this document may be illegible in electronic image products. Images are produced from the best available original document.

Simulation of Impact of the Generic Accident-Resistant Packaging (GAP)

Adam M. Slavin
Material and Structural Mechanics Department
Sandia National Laboratories
Albuquerque, New Mexico 87185

Abstract

Finite element simulations modelling impact of the Generic Accident-Resistant Packaging (GAP) have been performed. The GAP is a nuclear weapon shipping container that will be used by accident response groups from both the United States and the United Kingdom. The package is a thin-walled steel structure filled with rigid polyurethane foam and weighs approximately 5100 lbs when loaded. The simulations examined 250 ft/s impacts onto a rigid target at several orientations. The development of the finite element model included studies of modelling assumptions and material parameters. Upon completion of the simulation series, three full-scale impact tests were performed. A comparison of the simulation results to the test data is given. Differences between the results and data are examined, and possible explanations for the differences are discussed.

Acknowledgments

The support given to the simulation effort by Allen R. York, Org. 5165, is greatly appreciated. In addition, the PRONTO development team provided valuable assistance.

Table of Contents

List of Figures	6
List of Tables	7
1.0 Introduction	8
2.0 Description of the Generic Accident-resistant Packaging (GAP)	9
3.0 Finite Element Model Development	10
3.1 Simulation Code	10
3.2 Modelling the Containment Vessel (CV)	10
3.3 Modelling of the Double-Walled Outer Drum of the Overpack	10
3.4 Contact Surfaces	13
3.5 Complete Model	13
4.0 Material Properties	14
4.1 Material Properties of Metals	14
4.2 Rigid Polyurethane Foam Properties	14
5.0 Comparison of Simulation Results to the Test Data	17
5.1 Axial Impact	17
5.2 CG-Over-Corner Impact	19
5.3 Lateral Impact	22
5.4 Conclusions	24
6.0 References	25

List of Figures

Figure 1.	Schematic of the Generic Accident-resistant Packaging (GAP).	9
Figure 2.	Test model used to examine the effects of the outer drum wall modelling assumptions.	11
Figure 3.	Comparison of system response yielded by the single-walled and double-walled test models for the axial impact.	12
Figure 4.	Finite element mesh of the GAP.	13
Figure 5.	Comparison of test data to uniaxial crush response predicted by the Orthotropic Crush Model.	16
Figure 6.	Comparison of test data to hydrostatic crush response predicted by the Orthotropic Crush Model.	16
Figure 7.	Deformed shape of the GAP after the 250 ft/s axial impact.	18
Figure 8.	Comparison of predicted and measured G levels for the 250 ft/s axial impact...18	
Figure 9.	Measured dimensions of deformed CG-over-corner test unit.	19
Figure 10.	Deformed shape of the GAP after the 250 ft/s CG-over-corner impact.	20
Figure 11.	Comparison of predicted and measured G levels for the 250 ft/s CG-over-corner impact.	21
Figure 12.	Dimensions measure on the deformed lateral impact rest unit.	22
Figure 13.	Deformed shape of the GAP after the 250 ft/s lateral impact.	23
Figure 14.	Comparison of predicted and measured G levels for the 250 ft/s lateral impact. 23	

List of Tables

Table 1.	Metal Properties Used in the GAP Model	14
Table 2.	Measured and Predicted Dimensions of the Deformed CG-Over- Corner Impact Test Unit	19
Table 3.	Measured and Predicted Dimensions of the Deformed Lateral Impact Test Unit	22

1.0 Introduction

The H1636A Generic Accident-resistant Packaging (GAP) is a shipping container designed to hold a variety of nuclear weapons and weapon components. The package is a thin-walled steel structure filled with rigid polyurethane foam and weighs approximately 5100 lbs when loaded. The GAP will be used by accident response groups from both the United States and the United Kingdom and is intended to protect and contain the enclosed nuclear materials in impacts at speeds up to 250 ft/s.

To characterize the package response and to examine possible design improvements prior to fabrication of the packages, a three-dimensional finite element model of the system was developed, and simulations of package impact were performed. Development of the finite element model included validation of material constitutive models used in the simulation code and examination of a variety of modelling assumptions. The model was used to perform impact simulations at a variety of impact velocities and orientations.

Upon completion of the pre-test simulations, the package underwent four high speed impact tests to validate the design. Three of these tests were instrumented. These tests provided a rare opportunity to validate the finite element model. The predicted levels of crush, payload G levels, and rebound velocities were compared to the test data, and differences between the predicted results and the test data were examined.

2.0 Description of the Generic Accident-resistant Packaging (GAP)

A diagram of the GAP is shown in Figure 1. The GAP payload is a mockup of a weapon center-case. The mockup is enclosed in a containment vessel (CV) that must remain leak-tight after the impact in order to prevent the release of any nuclear material. The CV has a 0.38 in. thick 304 stainless steel wall stiffened with eight equally-spaced, axially-oriented 1x1x1/4 in. angle members. The mockup is supported by flexible and rigid foam, and is accessed through a lid in the CV that is attached with a tape joint. The CV is enclosed in an overpack consisting of concentric inner and outer drums separated by 20 lb (i.e., 20 lb/ft³) rigid polyurethane foam. The outer drum has a double wall of 0.06 in. thick 304 stainless steel. The outer drum is reinforced in the bottom with a 0.125 in. thick pan and around the center with a 0.125 in. thick hoop. The CV is accessed through a foam-filled lid insert that slides into the overpack and is held in place with two bolted lid plates. Two 0.25 in. thick aluminum load spreaders are embedded in the foam, one below the CV, and the other in the lid insert above the CV. The total weight of the system is approximately 5100 lb, 500 lb of which is the mockup payload weight.

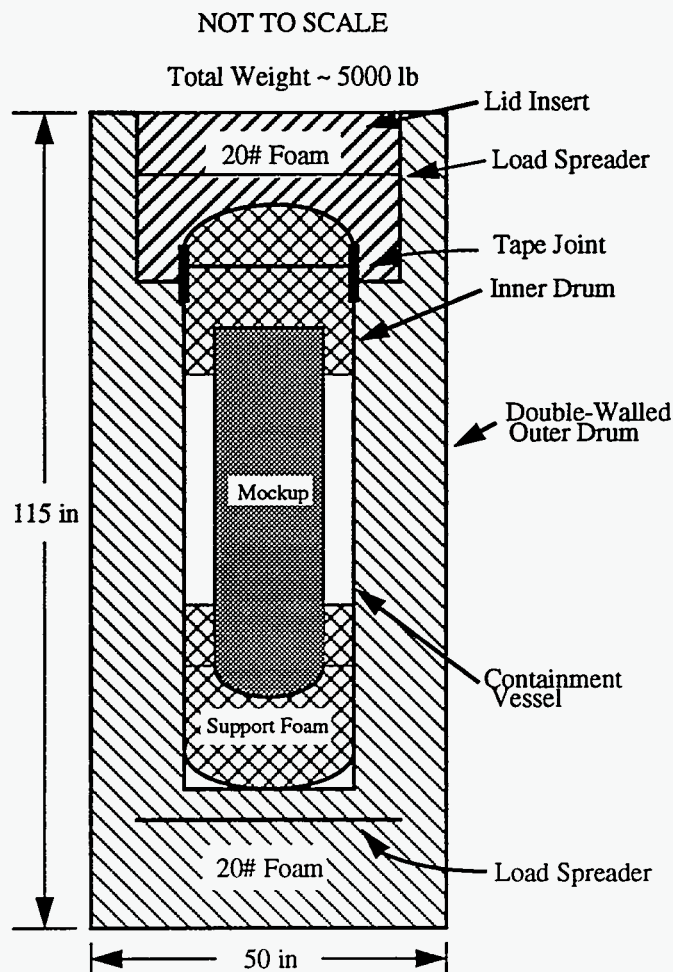


Figure 1. Schematic of the Generic Accident-resistant Packaging (GAP).

3.0 Finite Element Model Development

The pre-test GAP impact simulations were intended to provide estimates of strain levels in the containment vessel, the G levels experienced by the mockup, and levels of container crush. While no attempt was made to accurately predict tearing of the outer drum or lid-bolt failure, the simulations would provide qualitative predictions of drum and lid integrity. The system was therefore modelled with sufficient detail to provide this information as economically as possible. The rationale behind various modelling assumptions and the resulting limitations are described in detail in the following subsections.

3.1 Simulation Code

The impact simulations involve modelling nonlinear phenomena such as large deformations, nonlinear material response of metals and foams, and material self-contact. In addition, the combination of thin shell-like structures and regions of solid material in GAP necessitates use of both solid and shell type elements. The three-dimensional transient solid dynamics code PRONTO[1] was selected because it is well suited to handle these challenges.

3.2 Modelling the Containment Vessel (CV)

One of the goals of this study is to predict CV integrity. The system will be considered to have failed if the CV cracks, or if the tape joint fails, both of which imply a loss of containment. As an approximation of the CV response, the axially oriented stiffeners were not modelled. Instead, the stiffened region was thickened to provide equivalent stiffness. Because of the high computational costs that would be required, detailed modelling of the tape joint was not feasible for this type of study. As an approximation, the tape joint region was modelled to provide stiffness equivalent to that of the combined stiffness of the two layers of the actual joint.

3.3 Modelling of the Double-Walled Outer Drum of the Overpack

Upon impact of the system, the outer drum acts as a membrane, confining the foam as it is crushed. The response of the foam, which accounts for 40 percent of the system mass, and provides the vast majority of the energy-absorbing capability of the system, is significantly different for confined and unconfined crush. Therefore the membrane confinement provided by the drum greatly influences the overall response of the system. In addition to providing membrane confinement, the drum can also undergo bending, localized buckling and folding, and tearing.

Several factors affect the local buckling, bending, and membrane stiffnesses of the drum wall. The local buckling stiffness and the bending stiffness of the drum are related to the cube of the drum wall thickness, while the membrane stiffness of the drum is linearly related to the drum thickness. In addition, the local buckling stiffness of the outer drum as modelled in the finite element model is dependent on the size of the shell elements used to model the outer drum walls, and the constraints on the elements (i.e., whether or not the shell elements are attached to the solid elements used to model the foam). In the GAP, the foam is enclosed within the two concentric thin metal walls of the double-walled outer drum and can move relative to the drum walls. Such a condition is most closely approximated in a finite element model with a contact relation defined between the outer surface of the foam and the surface of the drum walls, which allows the drum walls to separate from the foam. In addition, if a sufficient number of elements are used to model the drum walls, the buckling and folding behavior can be closely approximated. With the further addition of

elements, tearing can also be simulated. However, this approach greatly increases the computational cost of the model. To capture only the membrane response of the drum wall, equivalent thickness shell elements are meshed directly to the foam. This reduces the model cost, but does not accurately capture the buckling or bending behavior of the outer drum.

To study the effect of the assumptions used in modelling the outer drum on the overall system response, simulations were performed with test models utilizing two different modelling approaches. In one model, both walls of the outer drum were modelled, and contact relations were defined between the outer walls and the foam. In the other model, the double-walled outer drum was modelled as a single, equivalent-thickness shell meshed directly onto the foam. The mass, dimensions, and impact velocity of the test models were similar to that of GAP (Figure 2 shows the double walled model).

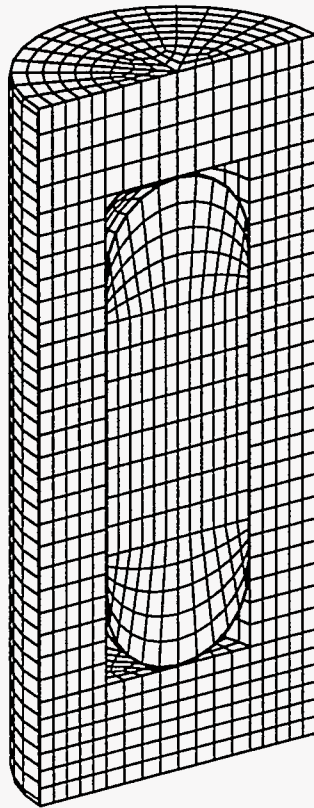


Figure 2. Test model used to examine the effects of the outer drum wall modelling assumptions.

To compare the effect of the outer drum on the system response, the maximum container crush, the mockup G levels, and the overall system kinetic energy were compared for the two models for both axial and lateral impact. Figure 3 compares the responses for the axial impact. For the lateral impact, the results yielded by the two models were virtually identical. The test simulations show that for the quantities of interest in the GAP impact simulations, detailed modelling of both walls of the outer drum is not necessary; a single, equivalent thickness shell meshed directly onto the foam is sufficient. Because this modelling approach greatly reduces the computational cost of the model, it was employed.

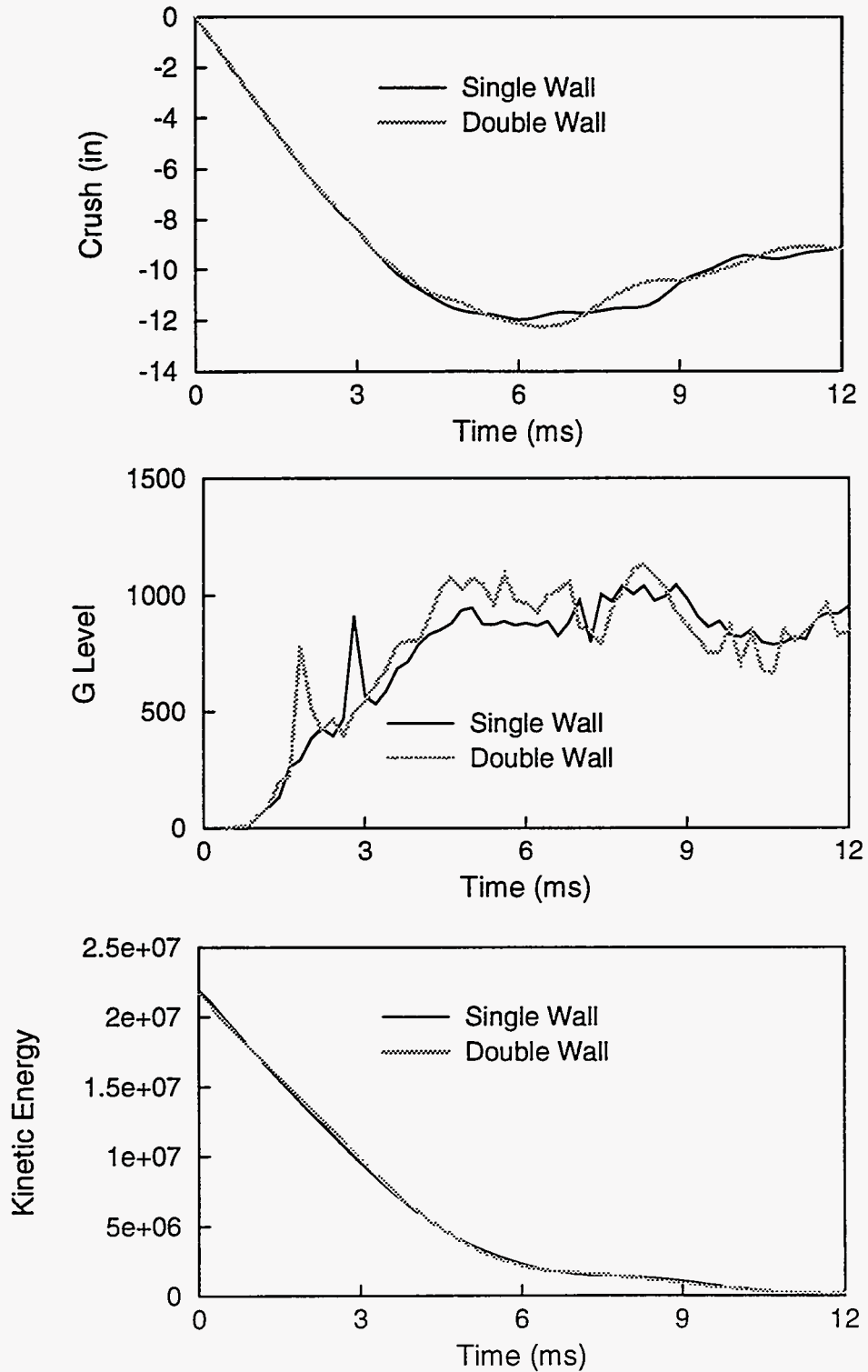


Figure 3. Comparison of system response yielded by the single-walled and double-walled test models for the axial impact.

3.4 Contact Surfaces

To allow the major components of the GAP to move relative to one another, contact relations were defined. The resulting model allows the lid and containment vessel to move relative to the drum overpack, and relative to one another. Within the containment vessel, the foam support closest to the lid can move relative to the vessel wall, and the mockup can move relative to both foam supports. The foam in the drum overpack was defined as a contact material to provide the self-contact capability required to allow it to fold up on itself during the extensive crushing experienced in the CG-over-corner impact.

3.5 Complete Model

The complete model included approximately 17,500 elements, with 13,200 8-noded hexagonal elements, and 4,300 four-noded quadrilateral shell elements. The model had a simulated weight of approximately 5000 lb, and required approximately 6 minutes of cpu time per millisecond of simulation. The finite element mesh is shown in Figure 4 (note: the lateral impact model had slightly more elements, and had a simulated weight of approximately 5150 lb because it included a more detailed representation of the lid).

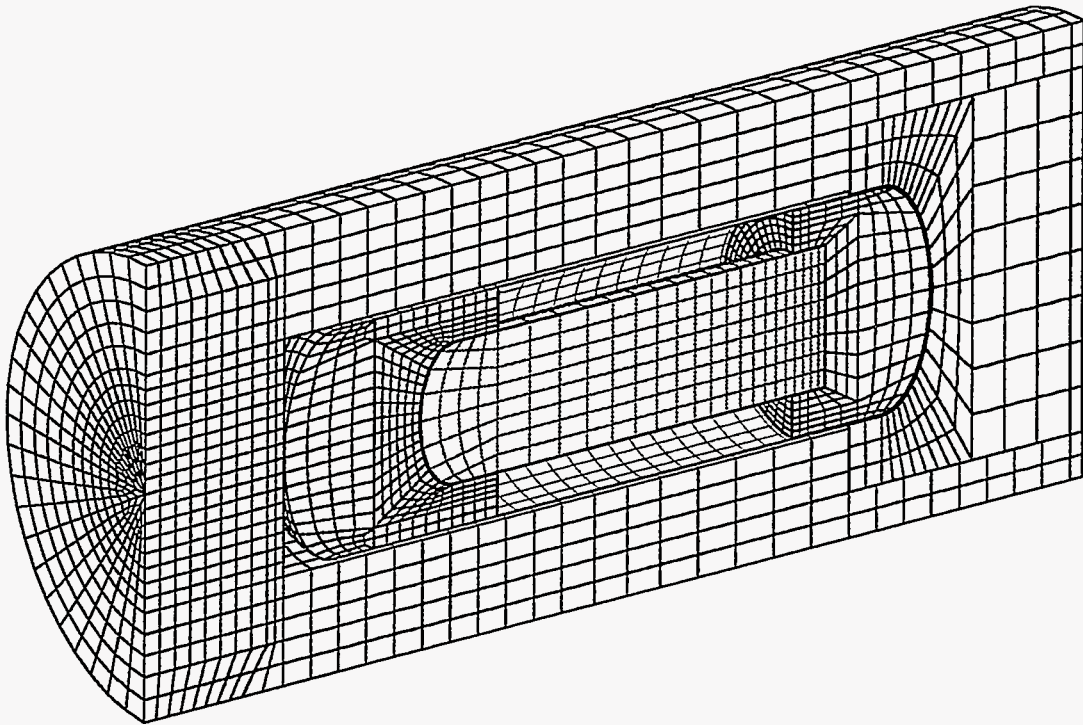


Figure 4. Finite element mesh of the GAP.

4.0 Material Properties

4.1 Material Properties of Metals

The stainless steel (containment vessel and drum) and the aluminum (load spreaders and mockup) were modelled as elastic/power law hardening materials using the EP POWER HARD constitutive model[3] implemented in PRONTO. The material constants are given below in Table 1. The modelled mockup was given a scaled density to match the weight of the actual mockup.

Table 1: Metal Properties Used in the GAP Model

Property	304 Stainless Steel	6061-T6 Aluminum
Density	0.3 lb/in ³	0.098 lb/in ³
Young's Modulus	28 Mpsi	9.9 Mpsi
Poisson's Ratio	0.27	0.33
Yield Stress	28 kpsi	42 kpsi
Hardening Constant	193 kpsi	29.9 kpsi
Hardening Exponent	0.7482	0.3406

4.2 Rigid Polyurethane Foam Properties

As mentioned above, the rigid polyurethane foam accounts for approximately 40 percent of the system mass, and for the majority of the energy-absorbing capacity of the system. It was therefore essential to validate the foam model and parameters used in the simulation. A study was performed to correlate finite element predictions yielded by the Orthotropic Crush Model[4] implemented in PRONTO with existing test data. The test data were obtained in unconfined uniaxial compression and hydrostatic compression tests of 20 lb foam (i.e., 20 lb per cubic foot) cube specimens by Lu, et al.[5].

As the name implies, the Orthotropic Crush Model can be used to model the crush response of orthotropic materials. The response of isotropic materials is modelled by using identical material properties for the three orthogonal material coordinate directions. The model divides the foam behavior into three regimes: elastic, volumetric crush, and fully compacted. In the elastic regime, the model assumes elastic behavior. In the volumetric crush regime, the stress is limited to a maximum value defined by strength versus volume curves. In the fully compacted regime, the material behaves as an elastic/perfectly plastic material.

The analysis model was a cube composed of 512 solid elements. The cube was compressed uniaxially by constraining all the nodes on a face of the cube and specifying a constant velocity to all of the nodes on the opposite face. The cubes were hydrostatically compressed by ramping up an equal pressure loading on all faces of the cube. Because the model does not include strain

rate dependence, the loading rate did not affect the results. Nevertheless, the response of polyurethane foam is strain rate dependent, therefore matching a material model to static data will affect the correlation between impact test data and simulation results.

PRONTO yields true stress and strain values. In contrast, the data are given in terms of engineering stress and strain. To compare the results to the test data, the stresses and strains were averaged over the whole model and then these single stress and strain values were converted to engineering stress and strain. Note that in the simulations, the specimen was compressed to 25 percent of its original height, showing slight hourglassing. The comparison of results to data for uniaxial loading is shown in Figure 5, and those for hydrostatic loading is shown in Figure 6.

Upon running the uniaxial and hydrostatic simulations and comparing the results to the test data, the values of the parameters were adjusted so the results were in better agreement with the data. It was necessary to reach a compromise fit of the data, as adjusting the parameters to attain better agreement with the uniaxial data degraded the agreement with the hydrostatic data. The material parameters for the Orthotropic Crush Model are described in detail in Ref.[4]. The input parameters for 20 lb foam are listed below in units of lbs. and inches.

Input Parameters: Orthotropic Crush Model, 20# Rigid Polyurethane Foam

```
MATERIAL, 100, ORTHOTROPIC CRUSH, 0.30E-4
MODULUS X, 33.0E3
MODULUS Y, 33.0E3
MODULUS Z, 33.0E3
MODULUS XY, 16.0E3
MODULUS YZ, 16.0E3
MODULUS ZX, 16.0E3
FULL COMPACTION, 0.63
COMPACTED YOUNGS MODULUS, 28.0E3
COMPACTED POISSONS RATIO, 0.35
COMPACTED YIELD STRESS, 17500.0
X ID, 1
Y ID, 1
Z ID, 1
XY ID, 2
YZ ID, 2
ZX ID, 2
END
```

```
FUNCTION, 1
0.02, 720.0
0.5, 2200.0
0.6, 3000.0
0.62, 3730.0
0.7, 5000.0
0.8, 8000.0
END
```

```
FUNCTION, 2, POLYNOMIAL
360.0, 0.0
1750.0
END
```

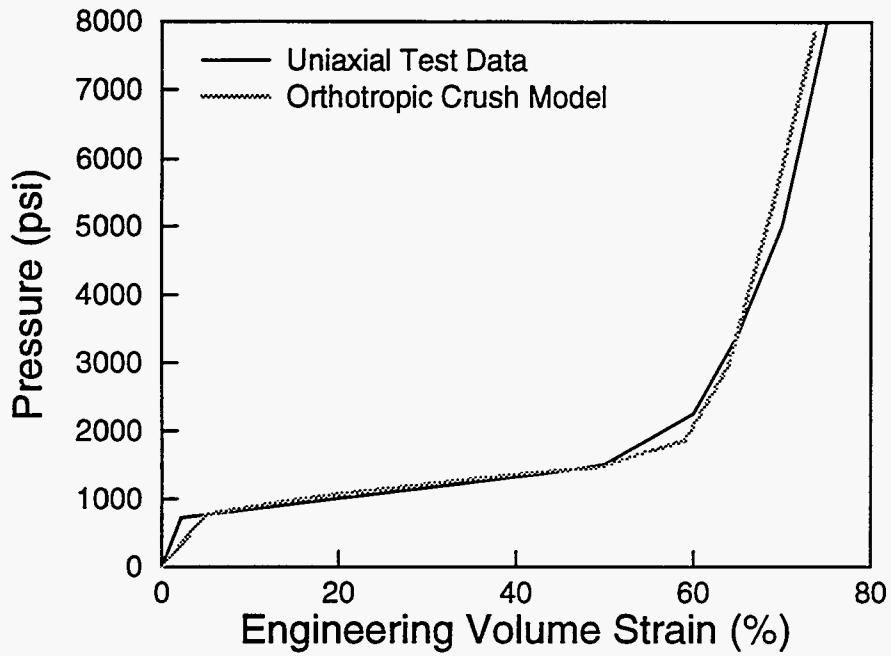



Figure 5. Comparison of test data to uniaxial crush response predicted by the Orthotropic Crush Model.

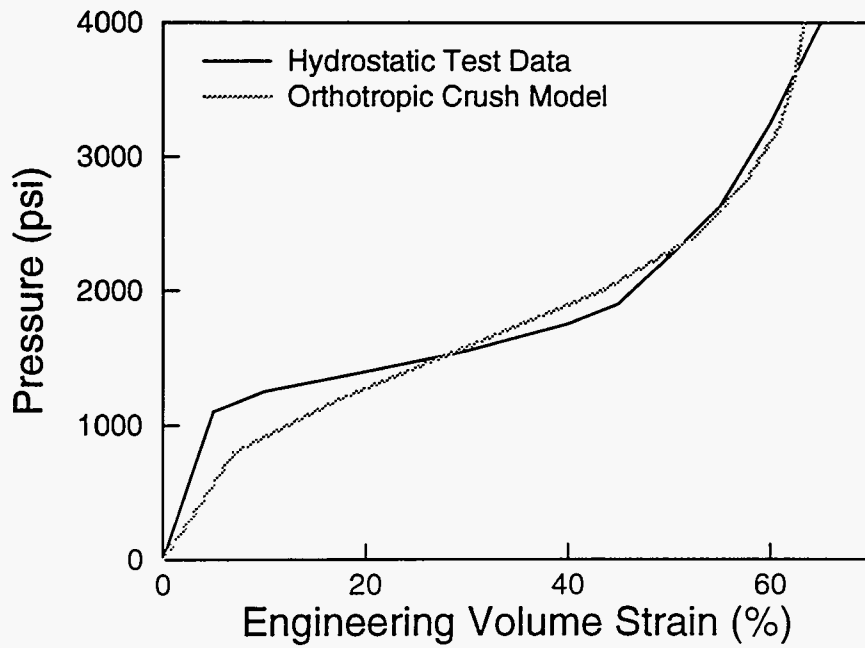


Figure 6. Comparison of test data to hydrostatic crush response predicted by the Orthotropic Crush Model.

5.0 Comparison of Simulation Results to the Test Data

As part of the pre-test characterization of the GAP design, axial, CG-over-corner, slapdown, and lateral simulations were performed at impact speeds of 44 ft/s, 250 ft/s, and 280 ft/s. Simulations were also performed to examine the effect of various design changes on the system response. The results and conclusions of the pre-test simulation study are documented in [6]. Tests were only performed at the 250 ft/s impact velocity. Therefore, the following discussion will only address the simulations corresponding to the 250 ft/s impact tests.

The impact orientations for the 250 ft/s tests were axial, CG-over-corner, and lateral. The tests were performed at the cable facility using rocket-driven pull-down. Separate test units were used, as the packages are significantly damaged in the impact. In the tests, the payload mockup was instrumented with fore and aft triaxial accelerometers, photometric records of the tests were taken, and the deformed packages were measured after the tests.

In the simulations, the plastic strain levels in the CV and the outer drum were monitored to qualitatively predict tearing or tape-joint failure, and the lid attachment was examined to determine if it would remain intact. Tearing was assumed to occur at 70 percent equivalent plastic strain in the 304 stainless steel[7]. In addition, deformations of the unit were measured, and the mockup G-level history and the rebound velocity of the container were monitored. The simulations were run until the container rebounded.

5.1 Axial Impact

The simulations predicted that the package would axially deform a maximum of 12 inches upon impact (Figure 7). The photometric data taken during the tests indicate that the package axially deformed approximately 17 inches. The simulations indicated that large scale tearing of the CV and drum was not likely. In the test, large scale tearing did not occur.

In determining the G level history of the payload mockup in the simulations, the axial accelerations of all the nodes in the mockup were summed and averaged. The history of this average value is compared in Figure 8 to the history of the average of the axial accelerations measured by the fore and aft accelerometers. The simulations closely approximated the initial G spike and closely predicted the duration and slope of the G pulse. However, the simulations overpredicted the maximum G levels by approximately 50 percent. Note also that the predicted G levels initially ramp up while the actual levels experience a more abrupt jump. This is probably caused by the closing of small tolerance gaps in the test unit, leading to a more abrupt loading of the payload. These gaps are not modelled in the simulations, and therefore, the predicted mockup G levels ramp up more gradually.

Finally, photometric measurements indicate that the rebound velocity of the package was approximately 55 ft/s. The analysis predicted a rebound velocity of 50 ft/s. This indicates that the simulations overpredicted the amount of energy absorbed during the impact by approximately 17 percent.

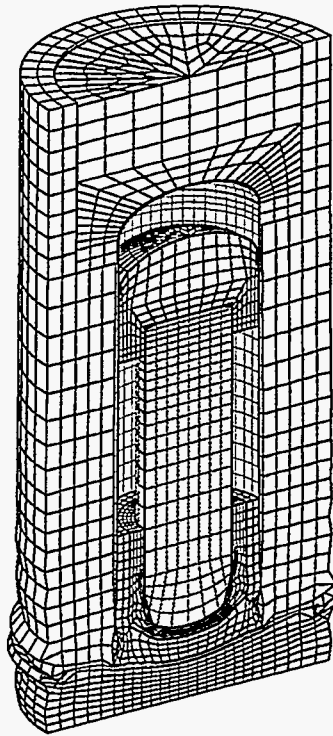


Figure 7. Deformed shape of the GAP after the 250 ft/s axial impact.

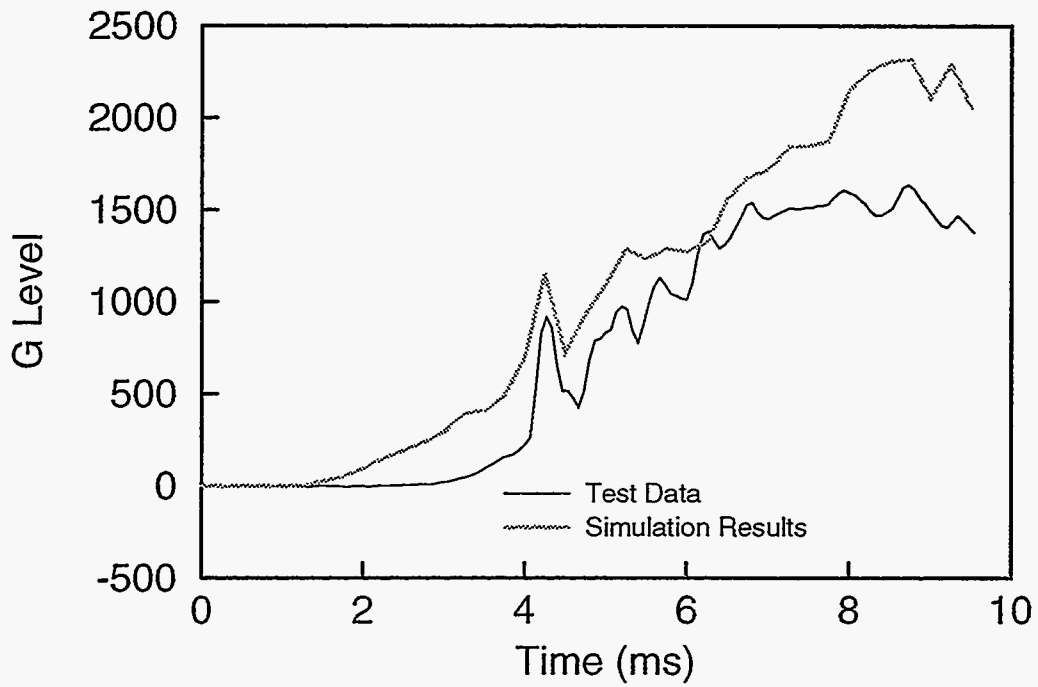


Figure 8. Comparison of predicted and measured G levels for the 250 ft/s axial impact.

5.2 CG-Over-Corner Impact

Table 2 compares the measured dimensions with those predicted by the simulations. Figure 9 shows the dimensions measured on the deformed CG-over-corner test unit. The deformed shape after the impact is shown in Figure 10. As seen in Figure 10, the upper section of mockup support foam was highly loaded along the aft edge of the mockup. The large deformation indicated that the support would probably be pulverized in this region, allowing the mockup to come loose. The test confirmed that the foam shattered in this region.

Table 2: Measured and Predicted Dimensions of the Deformed CG-Over-Corner Impact Test Unit

Dimension	Measured	Predicted
d1	102 in.	90 in.
d2	42 in.	39 in.
d3	3.5 in.	2.5 in.
d4	20 in.	17 in.
d5	124 in.	110 in.

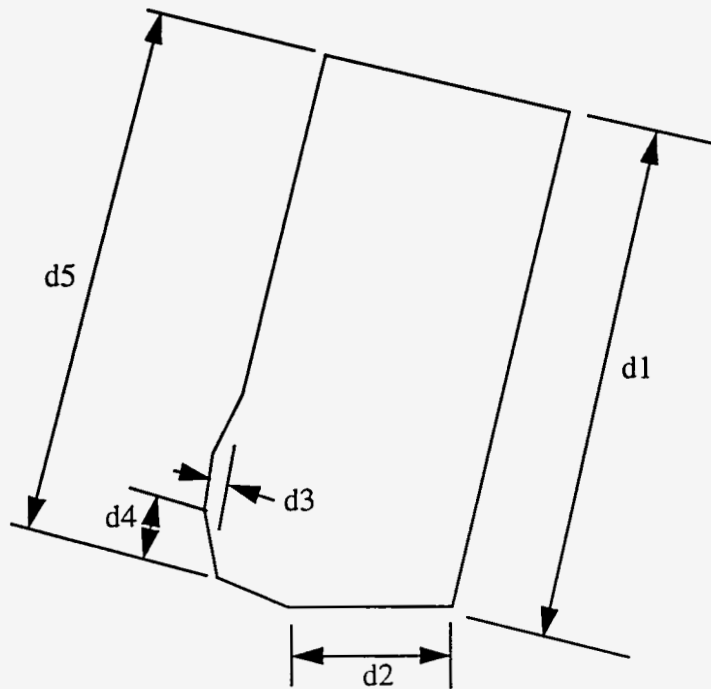


Figure 9. Measured dimensions of deformed CG-over-corner test unit.

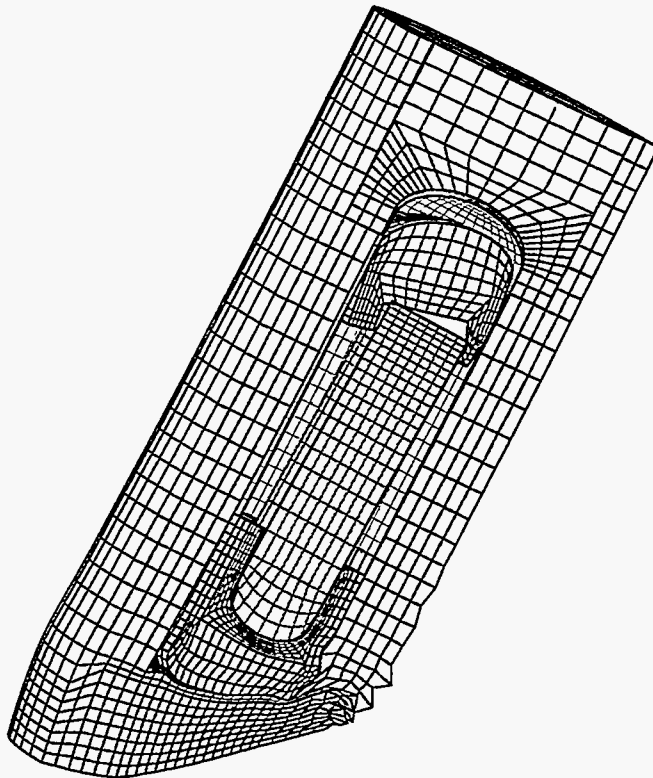


Figure 10. Deformed shape of the GAP after the 250 ft/s CG-over-corner impact.

The outer-most wall of the double-walled outer drum of the package circumferentially tore away from the top of the package. It is not apparent if the tearing was initiated by a flaw in the weld or was caused by the relatively massive pulldown hardware, which was not included in the model. This tearing was not predicted by the simulations. Note that the dimension d5 was 115 in. prior to impact and 124 in. after impact, indicating that the container lengthened upon impact. It is possible that after the outer wall tore loose it “telescoped” over the inner wall, making the package appear longer. However, this is not conclusive from the outside shape of the package. Furthermore, the package was not radiographed, so an internal view of the package is not available. Therefore it is inconclusive whether the simulations correctly predicted the amount of package crush. Finally, the simulations indicated that the CV would not tear. This was confirmed by the tests.

During fabrication, the foam is poured in 300 lb sections. These sections acted as independent units and tended to slide relative to one another during the impact because of the shearing induced by the off-axis loading. The sliding of the foam sections seen in the CG-over-corner impact was not apparent during the axial and lateral impacts because these impacts did not put a shear loading on the package.

Figure 11 compares the predicted and measured G levels experienced by the mockup during the CG-over-corner impact. The measured G levels are the square root of the sum of the squares of the average X, Y, and Z values from the fore and aft accelerometers. The predicted G levels are the square root of the sum of the squares of the averages of the X, Y, and Z nodal accelerations. Problems with the data acquisition system caused the beginning of the G level history to be lost, with the beginning of the recorded trace erroneously being placed at time zero. For comparison purposes, the measured G history was arbitrarily placed over the simulation results. The pulse shape and duration of the predicted and measured histories are quite similar. Again, the predicted G levels are higher than those measured, but only by about 15 percent.

The photometric measurements showed that the package rebounded with an angular velocity of approximately 3 rev/s. The simulations predicted 2.5 rev/s. It is difficult to compare energy absorption in this case because the package also had a small translational velocity component upon rebound, but this quantity proved difficult to measure from the photometric records. So while the simulations underpredicted the rotational energy of the package, the translational energy might have been overpredicted.

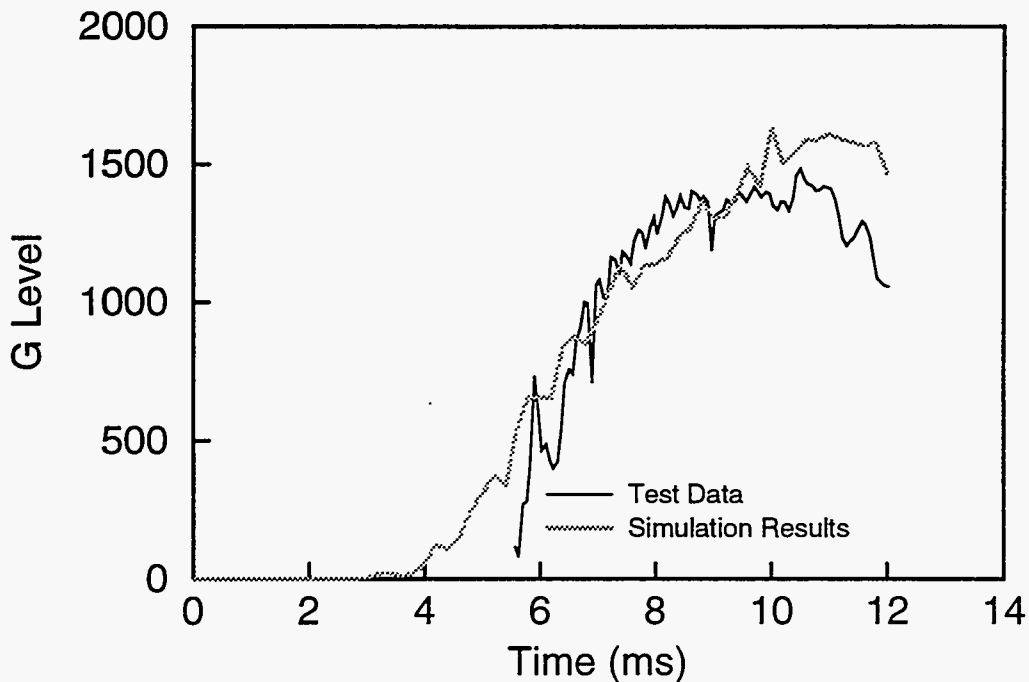


Figure 11. Comparison of predicted and measured G levels for the 250 ft/s CG-over-corner impact.

5.3 Lateral Impact

Table 3 compares the measured dimensions with those predicted by the simulations. Figure 12 shows the dimensions measured on the deformed unit. Note that the simulations are overpredicting the deformations.

Table 3: Measured and Predicted Dimensions of the Deformed Lateral Impact Test Unit

Dimension	Measured	Predicted
d1	45 in	42 in
d2	45 in	43 in
d3	39 in	37 in
d4	11 in	6 in

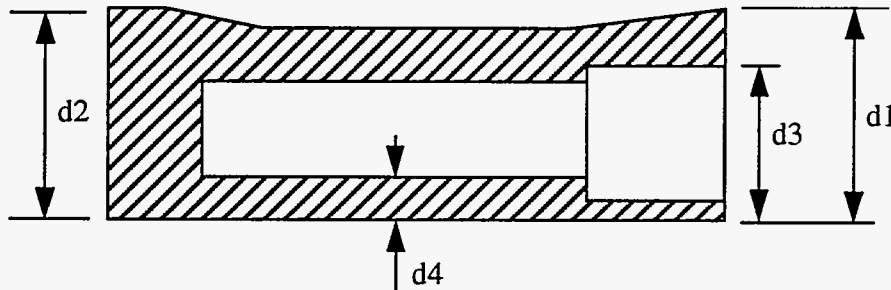


Figure 12. Dimensions measure on the deformed lateral impact rest unit.

Figure 13 shows the predicted deformed shape of the lateral impact test unit. The simulations indicated that the CV would undergo large deformations, but would not tear. In the test, the CV deformed appreciably without tearing. However, the tape joint region was bent, thereby unseating the O-ring seal and allowing a slow leak. This bending is evident in the predicted deformed shape of the CV. But, as mentioned above, the model is not sufficiently detailed to infer O-ring seal integrity.

Figure 14 shows a comparison of the measured and predicted G levels experienced by the mockup during the lateral impact. The trace of the predicted G levels significantly lagged behind the test data. Upon examination of the deformed shapes yielded by the simulations, it was noted that it took approximately 1.7 ms after impact for the containment vessel to contact the inner wall of the outer drum. This is because the containment vessel is modelled as “freely floating” in the outer package, and is therefore not in contact with the package at the instant of impact. The mockup does not experience any G loading until the containment vessel contacts the outer package. When the trace of the predicted G levels is shifted ahead 1.7 ms, the match between the data and the simulation results seen in Figure 14 is obtained. The pulse shape and duration are in good agreement, but the simulations overpredicted the G levels by approximately 30 percent.

Finally, the photometric data indicate that in the lateral impact, the package rebounded with a velocity of 40 ft/s. The simulation predicted a rebound velocity of 40 ft/s, indicating that the amount of energy absorbed upon impact was accurately predicted.

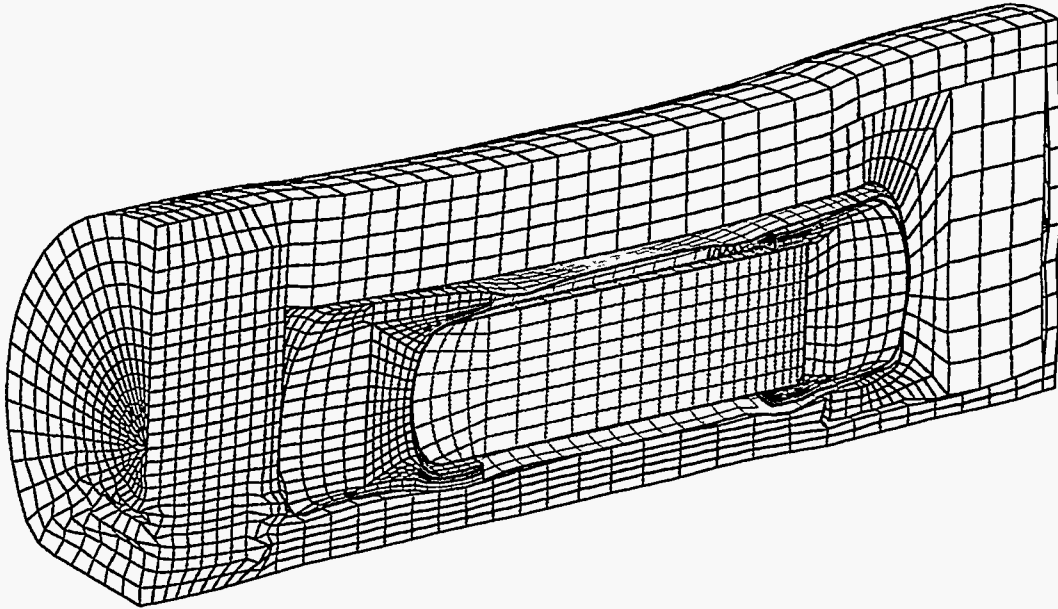


Figure 13. Deformed shape of the GAP after the 250 ft/s lateral impact.

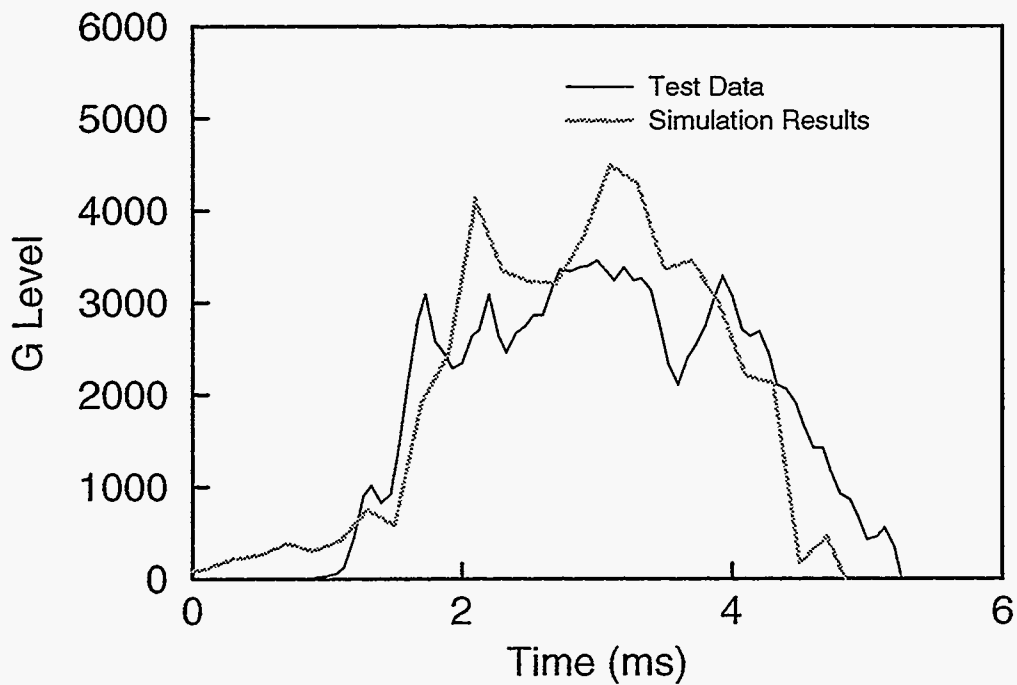


Figure 14. Comparison of predicted and measured G levels for the 250 ft/s lateral impact.

5.4 Conclusions

Overall, the agreement between the simulation results and the test data is quite good. Nevertheless, it is instructive to examine and attempt to explain the differences between the simulations and the data. This can ultimately lead to refinements in future models, enabling them to more accurately capture system response.

In any impact simulation, there will be differences between the results and the test data caused by simplifying assumptions used in constructing the simulation model. For example, it is difficult to characterize the friction acting in a system, so either friction is neglected, or the friction coefficients used are simply a “best guess.” In addition, simulation models typically assume perfect interfacial contact, where in actual systems, random imperfections and gaps exist. Furthermore, simulation models usually treat the target as infinitely rigid, when in fact the target will absorb some energy.

Because the GAP is composed largely of foam, it is expected that the system response would be largely governed by the foam response. Accordingly, the foam model was carefully validated. Yet the inconsistent crush response observed in the axial and lateral simulations (i.e., underprediction in the axial, overprediction in the lateral) indicate that the foam model might not be capturing all of the phenomena encountered in the test. Underprediction of crush could indicate that the foam constitutive model is overpredicting the stiffness of damaged foam. In the impact, the foam could be weakened as a result of damage, which is not modelled in the simulations. Damage was not present in the characterization tests described in [5], and is therefore not reflected in the data used to calibrate the constitutive model. Examination of the crushed foam inside the outer drum would determine whether damage is present and if the level of damage is significant. Overprediction of crush could be the result of strain-rate effects. Foam response is strain rate dependent, with the foam exhibiting greater strength with increased strain rate. The characterization tests were performed quasi-statically, and therefore do not reflect this strengthening. Using dynamic crush properties in the simulations would indicate whether strain rate effects contribute to the observed differences.

The simulation model tended to overpredict the mockup G levels. Overprediction of foam stiffness could contribute to the high G levels. The predicted G levels could also be affected by the assumptions used in modelling the containment vessel with equivalent thickness shells. This could be examined by modelling the containment vessel in greater detail and comparing its response to the equivalent thickness shell model.

Finally, future models could include refinements to more closely approximate the observed response. Contact surfaces could be used to represent the discrete foam sections. Also, future simulations could include the massive pulldown hardware, more refined meshes, and ductile failure models to better predict the observed tearing.

6.0 References

1. L. M. Taylor, D. P. Flanagan, *PRONTO 3D A Three-Dimensional Transient Solid Dynamics Program*, Sandia National Laboratories Report SAND87-1912, March 1989.
2. M. W. Heinstein, S. W. Attaway, J. W. Swegle, F. J. Mello, *A General-Purpose Contact Detection Algorithm for Nonlinear Structural Analysis Codes*, Sandia National Laboratories Report SAND92-2141, May 1993.
3. C. M. Stone, and G. W. Wellman, *A Vectorized Elastic/Plastic Power Law Hardening Material Model Including Luders Strain*, Sandia National Laboratories Report SAND90-0153, March 1990.
4. S. W. Attaway, *Orthotropic Crush Constitutive Relationship for PRONTO*, Sandia National Laboratories Internal Memorandum, September 29, 1992.
5. W. Y. Lu, J. S. Korellis, K. L. Lee, R. Grishaber, *Hydrostatic and Uniaxial Behavior of a High Density Polyurethane Foam (FR-3720) at Various Temperatures*, Sandia National Laboratories Report SAND93-8227, March 1993.
6. A. M. Slavin, *Pre-Test Impact Simulations of the Generic Accident-resistant Packaging (GAP)*, Sandia National Laboratories Internal Memorandum, March 15, 1994.
7. H. J. Rack, and G. A. Knorovsky, *An Assessment of Stress-Strain Data Suitable of Finite-Element Elastic-Plastic Analysis of Shipping Containers*, Sandia National Laboratories Report SAND77-1872, September 1978.

Distribution

MS0439	1434	D. R. Martinez
MS0841	1500	D. J. McCloskey
MS0828	1502	P. J. Hommert Route to: 1511
MS0441	1503	J. H. Biffle
MS0828	1504	E. D. Gorham Route to 1514, 1515
MS0834	1512	A. C. Ratzel Route to 1513,1516
MS0835	1513	R. D. Skocypec
MS0835	1513	J. L. Moya
MS0437	1516	F. J. Mello
MS0443	1517	H. S. Morgan
MS0443	1517	M. K. Neilsen
MS0437	1518	R. K. Thomas
MS0437	1518	S. W. Attaway
MS0437	1518	M. W. Heinstejn
MS0437	1518	A. M. Slavin (7)
MS0482	5161	R. E. Glass
MS0483	5165	R. L. Alvis
MS0483	5165	A. R. York(4)
MS0405	6411	D. D. Carlson
MS0717	6642	G. F. Hohnstreiter
MS9042	8741	G. A. Benedetti
MS9042	8741	M. L. Chièsa
MS9042	8742	J. L. Handrock
MS9042	8742	P. E. Nielan
MS9042	8742	L. I. Weingarten
MS9043	8743	M. L. Callabresi
MS0767	9603	E. R. Hoover
MS0492	12324	P. E. D'Antonio
MS0492	12332	G. A. Sanders
MS0491	12333	R. E. Smith
MS0899	13414	Technical Library (5)
MS0619	12613	Technical Publications
MS0100	7613-2	Document Processing for DOE/OSTI (2)
MS9018	8523-2	Central Technical Files